From Delay to Inertia and Triadic Interactions: A Reduction of Coupled Time-Delayed Oscillators

Lev A. Smirnov[1], Vyacheslav O. Munyayev[1], Maxim I. Bolotov[1], and Igor Belykh[2*]
[1]*Department of Control Theory, Lobachevsky State University of Nizhny Novgorod, 23 Gagarin Avenue, Nizhny Novgorod, 603022, Russia*
[2]*Department of Mathematics and Statistics and Neuroscience Institute, Georgia State University, P.O. Box 4110, Atlanta, Georgia, 30302-410, USA*
(Dated: December 12, 2025)

Time-delayed phase-oscillator networks model diverse biological and physical systems, yet standard first-order phase reductions cannot adequately capture their high-dimensional collective dynamics. In this Letter, we develop a second-order reduction for a broad class of time-delayed Kuramoto–Daido networks, transforming the original delayed system of one-dimensional phase oscillators into a delay-free network of two-dimensional rotators. The resulting model shows that coupling delay generates inertial terms in the intrinsic dynamics and higher-order (triadic) interactions, and it accurately predicts the emergence of complex collective patterns such as splay, cyclops, and chimera states. The reduction further reveals a qualitative division of roles: time delay acts primarily as effective inertia for higher-dimensional dynamics, including splay states, whereas the induced triadic interactions are decisive for lower-dimensional patterns such as chimeras. The method applies to networks with arbitrary topology, higher-harmonic coupling, and intrinsic-frequency heterogeneity, yielding a compact, parameter-explicit reduced model. This universal reduced description of time-delayed oscillator networks opens the door to systematic prediction and analysis of nontrivial collective dynamics in delay-coupled systems.

PACS numbers: 05.45.-a, 46.40.Ff, 02.50.Ey, 45.30.+s

Introduction. Networks of phase oscillators with time-delayed interactions provide a fundamental framework for collective dynamics in biological, physical, and technological systems with finite signal propagation speeds. A broad literature has shown that such delays can induce rich cooperative behavior, ranging from synchronization and bistability [1–8] to phase and amplitude chimeras, glassy phase-locked states and clustered chimera patterns [9–13], as well as twisted waves and related structured states [14, 15], delay-tunable multistability, and topology-dependent transitions [16, 17] in Kuramoto, phase-amplitude oscillator and spatially extended networks [18–21]. Comparable delay-induced phenomena have been documented in neuronal systems [22–30] and laser networks [31–33], where heterogeneous time delays can even generate robust disorder-induced phase locking of laser oscillators [34, 35].

Existing first-order reductions of time-delayed systems typically replace the delay by a static phase lag. While effective for synchronization and simple phase-locking [1–3], such reductions cannot adequately capture nontrivial collective states, such as splay, clustered, and chimera states, and their stability boundaries and basins of attraction. In the thermodynamic limit, the Ott–Antonsen ansatz [36] yields low-dimensional macroscopic reductions [8, 13, 14] which allow rigorous stability analysis, including delay-induced twisted states, but are restricted to purely first-harmonic coupling and specific choices of frequency and delay distributions. Second-order phase reductions have recently been developed for non-delayed [37–40] and delayed oscillator pairs [6], revealing how higher-order terms and amplitude variations shape transitions between phase-locked states; for delay-coupled Stuart–Landau oscillators, such expansions recover delay-dependent bistability and synchronization thresholds missed by first-order theory [7]. However, these approaches are formulated for low-dimensional systems and rely on conjugacy equations at the single-oscillator level, making them unsuitable for characterizing high-dimensional collective states, statistics, or basins in large networks. Thus, despite significant progress, we still lack a general predictive reduction for time-delayed phase oscillators that accommodates arbitrary topology, heterogeneous frequencies, and multi-harmonic coupling while remaining accurate for high-dimensional dynamics.

In this Letter, we close this gap and develop a second-order reduction for a broad class of time-delayed Kuramoto–Daido (KD) networks [41], transforming the original delayed system of one-dimensional (1D) phases into a delay-free network of two-dimensional rotators. The reduced model makes the effects of delay explicit through inertially augmented intrinsic dynamics and triadic phase interactions. It quantitatively reproduces complex collective states such as splay and chimera patterns in KD networks with time-delayed global and Kuramoto–Battogtokh–type nonlocal coupling [42]. We further show that the reduced model enables a constructive analysis of cyclops states [43]—a distinct class of three-

*Corresponding author, e-mail: ibelykh@gsu.edu

cluster generalized splay states—in networks with higher-harmonic coupling. Remarkably, the robust emergence of these cyclops states relies on genuinely two-dimensional intrinsic oscillator dynamics generated by delay-induced inertia, and is therefore inaccessible to standard first-order 1D phase reductions.

Time-delayed model and its second-order reduction. We study a generalized KD network with heterogeneous natural frequencies, external forcing, and time-delayed pairwise coupling:

$$\frac{d\theta_j(t)}{dt} = \varpi + \eta_j(t) + \frac{\varkappa}{N}\sum_{k=1}^{N} F_{jk}\big(\theta_k(t-\tau) - \theta_j(t)\big), \quad (1)$$

where $\theta_j(t)$ is the phase of oscillator j ($j = 1, \dots, N$), ϖ is a baseline (mean) natural frequency, $\eta_j(t)$ collects deviations from this baseline (including external forcing or detuning), $\varkappa$ is the coupling strength, and $F_{jk}(\cdot)$ are 2π-periodic pairwise coupling functions that may differ across oscillator pairs and represent, for example, random interactions. The parameter $\tau > 0$ is a uniform coupling delay. The results extend straightforwardly to heterogeneous node-wise delays τ_j, provided all incoming connections to node j share the same delay τ_j.

We analyze system (1) in the regime of weak frequency heterogeneity and coupling by introducing a small parameter $\varepsilon \ll 1$ so that $\eta_j(t) = \varepsilon\omega_j + \varepsilon\zeta_j(t)$, $\varkappa = \varepsilon\kappa$, where ω_j are small detunings from the baseline frequency ϖ and $\zeta_j(t)$ is a zero-mean time-dependent perturbation. In the limit $\varepsilon = 0$, all oscillators rotate uniformly with frequency ϖ. Treating ε as a small parameter, we perform a lengthy multiple–time-scale expansion to capture the slow modulation of phases by weak disorder and coupling (see the Supplementary Material for details). We introduce slow times $t_s = \varepsilon^s t$ ($s = 0, 1, 2, \dots$) and write

$$\theta_j(t) = \varpi t_0 + \phi_j(t_1, t_2, \dots) + \sum_{p=1}^{\infty} \varepsilon^p \varphi_j^{(p)}(t_0, t_1, t_2, \dots), \quad (2)$$

where ϖt_0 represents the leading-order, fast oscillatory behavior, ϕ_j describes the slow phase dynamics, and $\varphi_j^{(p)}$ are higher-order fast corrections that average out over the longer-term evolution of the system. Substituting (2) into (1), expanding the delayed terms, and eliminating secular contributions yields a solvability hierarchy in powers of ε. At $O(\varepsilon)$, we obtain the familiar delay-free KD phase model with a delay-induced phase shift [1]

$$\frac{d\phi_j}{dt} = \bar{\eta}_j(t) + \frac{\varkappa}{N}\sum_{k=1}^{N} F_{jk}\big(\phi_k - \phi_j - \varpi\tau\big), \quad (3)$$

where $\bar{\eta}_j(t) = \varepsilon\omega_j + \varepsilon\bar{\zeta}_j(t)$ is the averaged frequency perturbation. At $O(\varepsilon^2)$, the delay couples the slow time derivatives, and in the original time variable, the combined phase dynamics take the form of a second-order equation

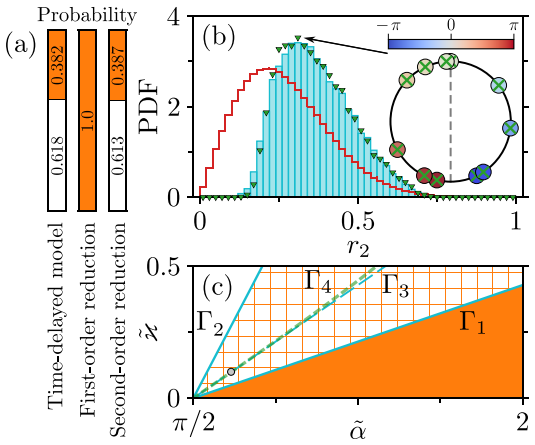

FIG. 1: (a) Probabilities of convergence to full synchrony (white) and generalized splay states (orange) for the time-delayed model with global, single-harmonic coupling and its first-order (3) and second-order (6) reductions, estimated from 5×10^4 simulations with random initial conditions (uniform phases; for the delayed system, random phase histories on $[-\tau, 0]$). (b) Probability density functions of $r_2 = |Z_2|$ for realized splay states in the time-delayed system (cyan histogram), compared with the first-order reduction (red curve) and the second-order reduction (green triangles). Parameters in (a,b): $N = 11$, $\varkappa = 0.1$, $\tau = 1$, $\varpi = 1$, $\alpha = 0.62$ (gray dot in (c)). (c) Stability regions of full synchrony (white) and splay states with $r_2 \le 0.8$ (orange) for the time-delayed model in the $(\tilde{\varkappa}, \tilde{\alpha})$ plane, where $\tilde{\varkappa} = \tau\varkappa$ and $\tilde{\alpha} = \alpha + \varpi\tau$. The hatched region indicates multistability of synchrony and generalized splay states. The solid cyan curves Γ_1 and Γ_2 are the stability boundaries for synchrony and splay states in the delayed system (the analytic curve Γ_1 corresponds to the condition $\tilde{\varkappa}^* = \tilde{\alpha} - \pi/2$, Γ_2 is obtained numerically). The dashed cyan curve Γ_3 and dashed green curve Γ_4 show the numerically computed stability boundaries for generalized splay states with $r_2 = 0$ in the delayed system and in the second-order reduced model (6), respectively.

$$\tau\frac{d^2\phi_j}{dt^2} + \frac{d\phi_j}{dt} = \left[\bar{\eta}_j(t) + \frac{\varkappa}{N}\sum_{k=1}^{N} F_{jk}\big(\Delta_{jk}\big)\right] \times \times \left[1 - \frac{\tau\varkappa}{N}\sum_{k=1}^{N} F'_{jk}\big(\Delta_{jk}\big)\right] + \tau\frac{d\bar{\eta}_j}{dt}, \quad (4)$$

where $\Delta_{jk} = \phi_k - \phi_j - \varpi\tau$. The reduced model (4) shows that the time delay τ manifests as an effective inertia, transforming the originally overdamped phase dynamics with time delay into a second-order system. The delay also generates higher-order (triadic) interactions: in Eq. (4), the second-order correction appears as a product of two sums, which yields a double sum corresponding to triplet couplings. This structure becomes particularly transparent for identical oscillators, where we set $\bar{\eta}_j(t) = 0$ (assumed hereafter) and consider single-harmonic coupling $F_{jk}(\vartheta) = G_{jk}\sin(\vartheta - \alpha)$ and $F'_{jk}(\vartheta) = G_{jk}\cos(\vartheta - \alpha)$, with G_{jk} denoting the coupling weights. Using trigonometric identities and the cancellation of antisymmetric double sums, Eq. (4) can be rewritten as

$$\tau\frac{d^2\phi_j}{dt^2}+\frac{d\phi_j}{dt}=\frac{\varkappa}{N}\sum_{k=1}^{N}G_{jk}\sin\left(\phi_k-\phi_j-\tilde{\alpha}\right)-$$
$$-\frac{\tau\varkappa^2}{2N^2}\sum_{k=1}^{N}\sum_{\ell=1}^{N}G_{jk}G_{j\ell}\sin(\phi_k+\phi_\ell-2\phi_j-2\tilde{\alpha}),\quad(5)$$

where $\tilde{\alpha}=\alpha+\varpi\tau$. The first sum corresponds to the standard pairwise Kuramoto–Sakaguchi coupling with a delay-induced phase shift. In contrast, the second sum is a purely delay-induced triadic interaction that couples oscillator j to phase triplets (j,k,ℓ). This structure mirrors the triplet interactions obtained via higher-order phase reduction for non-delayed Stuart–Landau oscillators [40], but here arises solely from memory (delay) without introducing amplitude degrees of freedom.

The reduced model (4) establishes a direct correspondence between time-delayed oscillator networks and inertial Kuramoto-type systems, making the memory effects of delay explicit in the effective dynamics. In what follows, we validate this reduction by comparing the second-order model (4), the first-order model (3), and the original delayed system under global, nonlocal, small-world, and two-harmonic coupling. We show that the second-order reduction accurately reproduces the statistics and dynamics of the time-delayed system (1), including coexistence of synchrony and splay states, the structure and prevalence of chimera patterns, and the emergence of cyclops cluster states, whereas the first-order model (3) systematically fails to capture these delay-induced regimes.

Global, one-harmonic coupling. We first test the reduced model (5) for single-harmonic mean-field coupling, $F_{jk}(\vartheta)=G_{jk}\sin(\vartheta-\alpha)$ with $G_{jk}=1$ for all j,k. Introducing the Kuramoto order parameters $Z_m=\sum_{k=1}^{N}e^{im\phi_k}/N$, Eq. (5) can be written in the compact mean-field form

$$\tau\frac{d^2\phi_j}{dt^2}+\frac{d\phi_j}{dt}=\varkappa\,\mathrm{Im}\left[Z_1e^{-i\psi_j}\right]-\frac{\tau\varkappa^2}{2}\mathrm{Im}\left[Z_1^2e^{-2i\psi_j}\right],\quad(6)$$

where $\psi_j=\phi_j+\tilde{\alpha}$ and $\tilde{\alpha}=\alpha+\varpi\tau$. Thus, delay induces an effective state-dependent second harmonic proportional to Z_1^2. For high-dimensional collective dynamics with small first-order parameter $r_1=|Z_1|\ll 1$ (e.g., generalized splay states [44]), the triadic term is negligible, and the delay acts primarily as effective inertia. In contrast, for lower-dimensional patterns such as chimera states with intermediate r_1, the triadic term becomes significant and encodes delay-induced higher-order correlations. The model (6) is analytically tractable. For generalized splay states $\phi_j=\phi_j^0=\text{const}$ with $Z_1=\sum_{k=1}^{N}e^{i\phi_k^0}/N=0$, Eq. (6) reduces to the Kuramoto model with inertia [44, 45]. The generalized splay-state stability condition derived in [43] can be written in terms of the parameters of (6) as $\tilde{\varkappa}<\tilde{\varkappa}^*=2\cos\tilde{\alpha}/(r_2^2-\sin^2\tilde{\alpha})$, for $|\sin\tilde{\alpha}|>r_2$, or $\tilde{\varkappa}>0$, for $\cos\tilde{\alpha}<-\sqrt{1-r_2^2}$, where $\tilde{\varkappa}=\tau\varkappa$ and $r_2=|Z_2|$ is the magnitude of the second Kuramoto moment. Similarly, linearizing (6) about the fully synchronous state $\phi_j=\varpi t$ yields the stability condition: $\tilde{\varkappa}>\tilde{\varkappa}^*=\cos\tilde{\alpha}/\cos(2\tilde{\alpha})$, for $|\sin\tilde{\alpha}|>1/\sqrt{2}$, or $\tilde{\varkappa}<\tilde{\varkappa}^*=\cos\tilde{\alpha}/\cos(2\tilde{\alpha})$, for $\cos\tilde{\alpha}>1/\sqrt{2}$, in agreement with classical necessary and sufficient condition [46]: $\varkappa F'(-\varpi_s\tau)>0$ obtained directly from the time-delayed system, up to terms of order $\tilde{\varkappa}^2$.

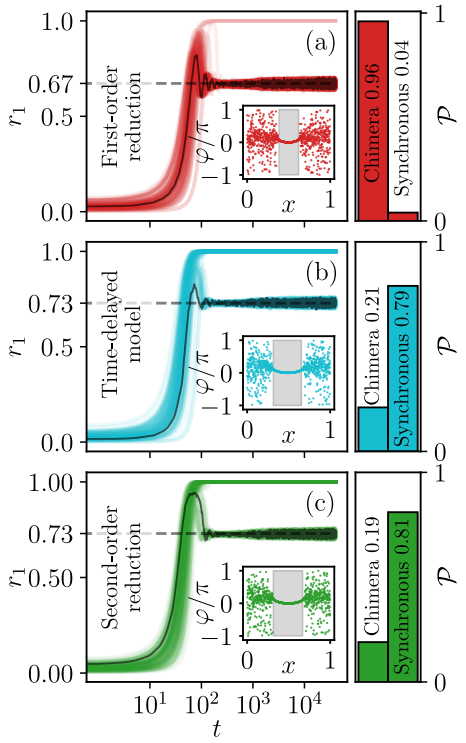

FIG. 2: Dynamics of the order parameter r_1 for the time-delayed system (1) with Kuramoto–Battogtokh nonlocal coupling (central panel), compared with the first-order reduction (3) (top) and the second-order reduction (6) (bottom). Each panel shows results from 250 simulations with random initial phases $\phi_j(0)\in[-\pi,\pi]$ (and zero initial velocities $\dot{\phi}_j(0)=0$ for the second-order model). The black curve highlights a representative chimera trajectory; the inset shows the corresponding phase distribution $\varphi_j=\phi_j-\phi_{N/2}$ aligned to the central oscillator, with the gray band indicating the synchronized cluster. Right panels display the probabilities $\mathcal{P}$ of convergence to full synchrony and to chimera states. Parameters: $N=1024$, $L=1.0$, $\kappa=5.2$, $\tau=0.08$, $\varpi=5.125$, $\alpha=1.047$.

Figure 1(a,b) tests the predictive power of the second-order model (6) by comparing it with the original delayed system (1) and the first-order reduction (3). Figure 1(a) shows that the second-order model reproduces the statistics of the delayed system almost perfectly, whereas the first-order model misestimates these probabilities and frequently misses the synchronous state altogether. Figure 1(b) compares probability density functions (PDFs) of generalized splay states at fixed r_2: the PDFs (and the individual phase configurations, inset) from the second-order and delayed models coincide, while

the first-order reduction exhibits a pronounced bias. Figure 1(c) presents the stability diagram of synchrony and generalized splay states in terms of $\tilde{\varkappa} = \tau\varkappa$ and $\tilde{\alpha} = \alpha + \varpi\tau$. For generalized splay states with $r_2 = 0$, the numerical stability curves Γ_3 (the delayed system) and Γ_4 (second-order system) begin to diverge around $\tilde{\varkappa} \approx 0.5$, indicating the range of quantitative validity of the second-order approximation. Since the effective expansion parameter is $\tilde{\varkappa} = \tau\varkappa$, small delays permit relatively strong coupling, while weak coupling allows predictive use of the reduced model even for comparatively large delays.

Nonlocal Kuramoto-Battogtokh coupling. To highlight the power and generality of the second-order reduction, we apply it to what is arguably a stringent testbed: the time-delayed system (1) with Kuramoto–Battogtokh–type nonlocal coupling, which supports chimera states whose shape is highly sensitive to approximation [47]. We consider identical oscillators arranged at equal intervals on a ring segment of length L, with positions $x_j = jL/N$. The nonlocal coupling is defined by the exponential kernel [42, 47]: $G(x) = \kappa\cosh(\kappa\,|x|)\big/2\sinh(\kappa L/2)$, and the coupling functions $F_{jk}\big(\phi_k(t-\tau)-\phi_j(t)\big) = G_{jk}\sin\big(\phi_k(t-\tau)-\phi_j(t)-\alpha\big)$ with phase shift α and coupling coefficients $G_{jk} = G(x_k - x_j)$. Figure 2 compares the dynamics of the delayed Kuramoto–Battogtokh system with its first- and second-order reductions. For 250 random initial conditions, the time series of the order parameter r_1 in the second-order model closely reproduces the ensemble of trajectories of the delayed system, including the characteristic chimera branch (black curve), while the first-order reduction yields clearly distorted r_1 dynamics and often fails to reach full synchrony. The inset shows that the phase profile of a representative chimera, such as its cluster size and shape of the synchronized domain, matches almost perfectly between the delayed system and the second-order reduction. In contrast, the first-order model produces a visibly different pattern. The probability panels on the right confirm this claim quantitatively: the second-order model captures the coexistence statistics of fully synchronous and chimera states observed in the delayed system, while the first-order reduction both underestimates full synchronization and misidentifies the prevalence of chimera states.

Small-world network. We also tested the reduction in a more demanding setting: a Watts–Strogatz small-world network [48] with the time-delayed coupling function $F_{jk}\left(\phi_k(t-\tau)-\phi_j(t)\right) = A_{jk}\sin\left(\phi_k(t-\tau)-\phi_j(t)\right)$, where $A_{jk} = Na_{jk}/\kappa_j$, κ_j is the degree of node j, and a_{jk} form the adjacency matrix shown in Fig. 3(a). This network supports twisted states [14, 41], i.e., partially synchronous patterns in which the phases wind nontrivially around the circle and form nonuniform spatial profiles. Figure 3 shows that the second-order reduced model reproduces these inhomogeneous twisted states with high accuracy, both in the time series of the order parameter and in the instantaneous phase and phase-density profiles, while also matching the coexistence statistics of twisted and more synchronized regimes obtained from the full delayed system. In contrast, the first-order reduction yields noticeably different statistics and distorted twisted-state profiles, underscoring again that delay-induced inertial and triadic terms are essential for capturing the collective dynamics in complex network topologies.

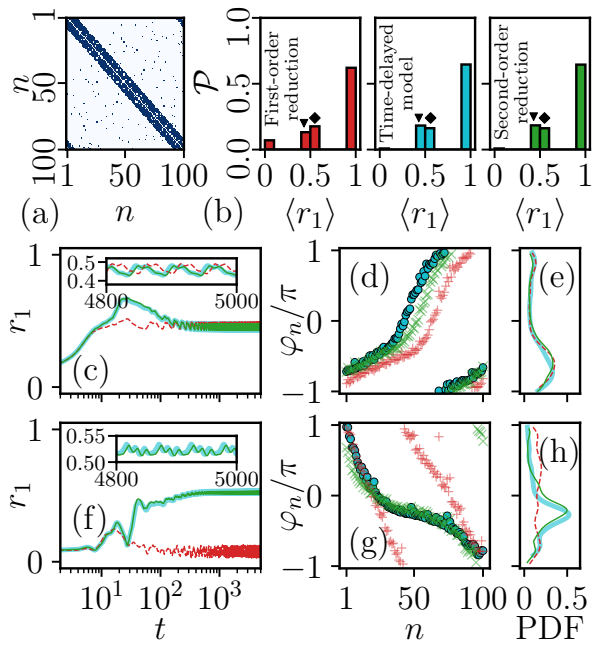

FIG. 3: (a) Adjacency matrix of the time-delayed small-world network ($N = 100$, mean degree $\langle\kappa\rangle = 16$, rewiring probability $p = 0.08$). (b) Probabilities $\mathcal{P}$ of realizing different stable regimes for random initial conditions in the delayed network and in the corresponding first- and second-order reduced models (2,000 runs; initial phases drawn as random constants). Triangle and diamond markers indicate bins corresponding to the examples shown in (d) and (g). (c,f) Time series of the order parameter r_1 for selected regimes, comparing the delayed system (cyan), the second-order reduction (green), and the first-order reduction (red) under identical initial conditions. (d,g) Instantaneous phase snapshots, and (e,h) phase-density profiles (PDFs), illustrating partially synchronous nonuniform twisted states. Parameters: $\varkappa = 0.05$, $\varpi = 0.94$, $\tau = 1$.

Global bi-harmonic coupling. As a further test of the reduction framework in a challenging setting with a richer coupling structure, we consider globally coupled oscillators with bi-harmonic interactions, $F_{jk}\big(\phi_k(t-\tau) - \phi_j(t)\big) = \sum_{q=1}^{2} K_q\sin\big(\phi_k(t-\tau) - \phi_j(t) - \alpha_q\big)$, where K_q and α_q are the strength and phase shift of the q-th harmonic. The second-order reduction yields (4) with the bi-harmonic coupling and is capable of capturing cyclops

states [43] – three-cluster generalized splay states composed of two coherent clusters and a solitary oscillator – as well as their nonstationary breathing and switching variants [49, 50]. In this regime, the delay-induced inertial term and the resulting two-dimensional intrinsic dynamics are essential: cyclops states are prevalent attractors in the delayed system and in the second-order model, yet remain essentially invisible to the first-order (1D) reduction, which fails to capture their nearly global basins of attraction. Figure 4 illustrates that the second-order reduction faithfully reproduces not only stationary but also nonstationary cluster dynamics in the bi-harmonic case. For representative parameter sets, the reduced model tracks the time evolution of the order parameters r_1 and r_2, and the instantaneous phase configurations of stationary, breathing, and switching cyclops states with high accuracy, demonstrating that it accurately captures even strongly non-stationary cluster dynamics in the delayed bi-harmonic regime.

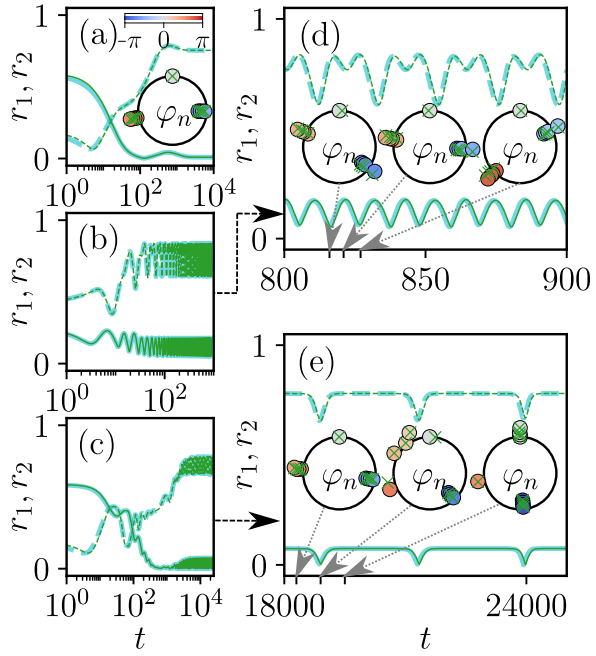

FIG. 4: Cyclops, breathing and switching cyclops states in the delayed bi-harmonic KD model (cyan) and its second-order reduction (green). Panels show the time evolution of the first (r_1, solid) and second (r_2, dashed) Kuramoto order parameters for (a) a stationary cyclops state ($\alpha_1 = 1.9$, $\alpha_2 = -2.4$), (b,d) a breathing cyclops state ($\alpha_1 = 0.42$, $\alpha_2 = -2.3$), and (c,e) a switching cyclops state ($\alpha_1 = 0.6$, $\alpha_2 = -0.92$). Insets in (a,d,e) display instantaneous phase snapshots for the delayed system (colored circles) and the second-order reduction (crosses), illustrating the match of cluster structure and solitary oscillator position. Initial conditions are uniformly random constant phases. Parameters: $N = 9$, $\tau = 1$, $\varkappa = 0.1$, $K_1 = 10$, $K_2 = 0.5$, $\varpi = 1.2$.

Conclusions. We have developed a universal second-order reduction for time-delayed KD networks that maps delayed 1D phase dynamics to a delay-free network of 2D rotators. This framework establishes a rigorous link between delay-induced memory and effective inertia plus higher-order (triadic) interactions, providing an analytically tractable, compact, and parameter-explicit model for delayed oscillator ensembles. Across global, nonlocal, and small-world topologies and biharmonic coupling, the second-order reduction nearly perfectly reproduces the emergence statistics and shapes of complex, possibly nonstationary patterns, whereas first-order reductions fail to do so. Taken together, these results indicate that the second-order reduction provides an optimal balance: it is sufficiently high-order to encode the key delay-induced mechanisms, yet remains low-dimensional enough to be analytically transparent and computationally efficient, without requiring higher-order (e.g., third-order) corrections. Notably, our reduction shows that, in the weak-coupling regime, the time-delayed 1D Kuramoto model (as a particular case of the KD setting) is dynamically equivalent to a delay-free 2D Kuramoto-type model with inertia (and additional higher-order interaction terms, where applicable). This mapping provides an independent validation and a new application domain for inertial Kuramoto models, extending their relevance beyond their established roles as effective descriptions of adaptive-frequency firefly synchronization [51], power-grid oscillator networks [52]], and theta-neuron populations with adaptive synaptic coupling [30, 43]. Because many physical and biological systems with delays, such as networks of integrate-and-fire neurons [53] , Josephson junction arrays [54–56], and laser oscillators with delayed feedback [34, 57], can be reduced to KD-type phase dynamics, the present reduction offers a broadly applicable tool for predicting and designing delay-controlled collective behavior in real-world oscillator networks.

Acknowledgments. We are grateful to G.V. Osipov for valuable discussions. This work was supported by the RSF under Project No. 22-12-00348-P (to V.O.M., and M.I.B.), the MSHE under Project No. FSWR-2024–0005 (to L.A.S., Supplemental Material), and the National Science Foundation (USA) under grant DMS-2510860 (to I.B.).

[1] E. M. Izhikevich, Physical Review E **58**, 905 (1998).
[2] M. S. Yeung and S. H. Strogatz, Physical Review Letters **82**, 648 (1999).
[3] M. G. Earl and S. H. Strogatz, Physical Review E **67**, 036204 (2003).
[4] D. J. Jörg, L. G. Morelli, S. Ares, and F. Jülicher, Physical Review Letters **112**, 174101 (2014).
[5] J. G. Restrepo and P. S. Skardal, Physical Review Research **1**, 033042 (2019).
[6] J. L. Ocampo-Espindola, I. Z. Kiss, C. Bick, and K. C.

Wedgwood, Physical Review Research **6**, 033328 (2024).
[7] C. Bick, B. Rink, and B. A. de Wolff, arXiv preprint arXiv:2404.11340 (2024).
[8] W. S. Lee, E. Ott, and T. M. Antonsen, Physical Review Letters **103**, 044101 (2009).
[9] C. Bick, M. Sebek, and I. Z. Kiss, Physical Review Letters **119**, 168301 (2017).
[10] S. Ameli, M. Karimian, and F. Shahbazi, Chaos: An Interdisciplinary Journal of Nonlinear Science **31** (2021).
[11] A. Gjurchinovski, E. Schöll, and A. Zakharova, Physical Review E **95**, 042218 (2017).
[12] J. H. Sheeba, V. Chandrasekar, and M. Lakshmanan, Physical Review E—Statistical, Nonlinear, and Soft Matter Physics **79**, 055203 (2009).
[13] W. S. Lee, J. G. Restrepo, E. Ott, and T. M. Antonsen, Chaos: An Interdisciplinary Journal of Nonlinear Science **21**, 023122 (2011).
[14] C. R. Laing, Chaos: An Interdisciplinary Journal of Nonlinear Science **26**, 094802 (2016).
[15] Y.-H. An, M.-S. Ho, R.-S. Kim, and C.-U. Choe, Physica D: Nonlinear Phenomena **464**, 134204 (2024).
[16] J. Sawicki, I. Omelchenko, A. Zakharova, and E. Schöll, The European Physical Journal Special Topics **226**, 1883 (2017).
[17] H. Wu and M. Dhamala, Physical Review E **98**, 032221 (2018).
[18] M. Wolfrum and S. Yanchuk, Physical Review Letters **96**, 220201 (2006).
[19] G. C. Sethia, A. Sen, and F. M. Atay, Physical Review Letters **100**, 144102 (2008).
[20] S. Ares, L. G. Morelli, D. J. Jörg, A. C. Oates, and F. Jülicher, Physical Review Letters **108**, 204101 (2012).
[21] S. Yanchuk and G. Giacomelli, Physical Review Letters **112**, 174103 (2014).
[22] M. Dhamala, V. K. Jirsa, and M. Ding, Physical Review Letters **92**, 074104 (2004).
[23] X. Sun, M. Perc, and J. Kurths, Chaos: An Interdisciplinary Journal of Nonlinear Science **27**, 053113 (2017).
[24] J. Lehnert, T. Dahms, P. Hövel, and E. Schöll, Europhysics Letters **96**, 60013 (2011).
[25] O. V. Popovych, S. Yanchuk, and P. A. Tass, Physical Review Letters **107**, 228102 (2011).
[26] A. Keane, T. Dahms, J. Lehnert, S. A. Suryanarayana, P. Hövel, and E. Schöll, The European Physical Journal B **85**, 407 (2012).
[27] J. Sawicki, I. Omelchenko, A. Zakharova, and E. Schöll, The European Physical Journal B **92**, 54 (2019).
[28] J. Sawicki, S. Ghosh, S. Jalan, and A. Zakharova, Frontiers in Applied Mathematics and Statistics **5**, 19 (2019).
[29] A. Lucchetti, M. H. Jensen, and M. L. Heltberg, Physical Review Research **3**, 033041 (2021).
[30] L. A. Smirnov, V. O. Munyayev, M. I. Bolotov, G. V. Osipov, and I. Belykh, Frontiers in Network Physiology **4**, 1423023 (2024).
[31] G. Kozyreff, A. Vladimirov, and P. Mandel, Physical Review Letters **85**, 3809 (2000).
[32] J. D. Töpfer, H. Sigurdsson, L. Pickup, and P. G. Lagoudakis, Communications Physics **3**, 2 (2020).
[33] S. Heiligenthal, T. Dahms, S. Yanchuk, T. Jüngling, V. Flunkert, I. Kanter, E. Schöll, and W. Kinzel, Physical Review Letters **107**, 234102 (2011).
[34] N. Nair, K. Hu, M. Berrill, K. Wiesenfeld, and Y. Braiman, Physical Review Letters **127**, 173901 (2021).
[35] A. E. D. Barioni, A. N. Montanari, and A. E. Motter, Physical Review Letters **135**, 197401 (2025).
[36] E. Ott and T. M. Antonsen, Chaos: An Interdisciplinary Journal of Nonlinear Science **18**, 037113 (2008).
[37] M. Rosenblum and A. Pikovsky, Chaos: An Interdisciplinary Journal of Nonlinear Science **29**, 011105 (2019).
[38] E. T. Mau, M. Rosenblum, and A. Pikovsky, Chaos: an Interdisciplinary Journal of Nonlinear Science **33**, 10101 (2023).
[39] E. Gengel, E. Teichmann, M. Rosenblum, and A. Pikovsky, Journal of Physics: Complexity **2**, 015005 (2020).
[40] E. T. Mau, O. E. Omelchenko, and M. Rosenblum, Physical Review E **110**, L022201 (2024).
[41] J. A. Acebrón, L. L. Bonilla, C. J. P. Vicente, F. Ritort, and R. Spigler, Reviews of Modern Physics **77**, 137 (2005).
[42] L. Smirnov, G. Osipov, and A. Pikovsky, Journal of Physics A: Mathematical and Theoretical **50**, 08LT01 (2017).
[43] V. O. Munyayev, M. I. Bolotov, L. A. Smirnov, G. V. Osipov, and I. Belykh, Physical Review Letters **130**, 107201 (2023).
[44] R. Berner, S. Yanchuk, Y. Maistrenko, and E. Scholl, Chaos: An Interdisciplinary Journal of Nonlinear Science **31**, 073128 (2021).
[45] V. O. Munyayev, M. I. Bolotov, L. A. Smirnov, G. V. Osipov, and I. V. Belykh, Physical Review E **105**, 024203 (2022).
[46] M. G. Earl and S. H. Strogatz, Physical Review E **67**, 036204 (2003).
[47] Y. Kuramoto and D. Battogtokh, Nonlinear Phenomena in Complex Systems **5**, 380 (2002).
[48] D. J. Watts and S. H. Strogatz, Nature **393**, 440 (1998).
[49] M. I. Bolotov, V. O. Munyayev, L. A. Smirnov, G. V. Osipov, and I. Belykh, Physical Review E **109**, 054202 (2024).
[50] M. I. Bolotov, L. A. Smirnov, V. O. Munyayev, G. V. Osipov, and I. Belykh, Physical Review E **112**, L052202 (2025).
[51] B. Ermentrout, Journal of Mathematical Biology **29**, 571 (1991).
[52] L. Tumash, S. Olmi, and E. Schöll, Chaos: An Interdisciplinary Journal of Nonlinear Science **29**, 123105 (2019).
[53] W. Gerstner and W. M. Kistler, *Spiking Neuron Models: Single Neurons, Populations, Plasticity* (Cambridge University Press, 2002).
[54] K. Wiesenfeld, P. Colet, and S. H. Strogatz, Physical Review Letters **76**, 404 (1996).
[55] K. Wiesenfeld, P. Colet, and S. H. Strogatz, Physical Review E **57**, 1563 (1998).
[56] B. R. Trees, V. Saranathan, and D. Stroud, Physical Review E **71**, 016215 (2005).
[57] B. Garbin, J. Javaloyes, G. Tissoni, and S. Barland, Nature Communications **6**, 5915 (2015).